

# Analysing the innermost dust in Seyfert nuclei with the Keck Interferometer: the particular case of NGC 4151

Jorg-Uwe Pott<sup>1,2,3</sup>, Matt A. Malkan<sup>2</sup>, Moshe Elitzur<sup>4</sup>, Andrea M. Ghez<sup>2,5</sup>, Tom M. Herbst<sup>1</sup>,  
Rainer Schödel<sup>6</sup>, Julien Woillez<sup>3</sup>

## ABSTRACT

After recent sensitivity upgrades at the Keck Interferometer (KI), systematic interferometric  $2\ \mu\text{m}$  studies of the innermost dust in nearby Seyfert nuclei are within observational reach. Here we present the analysis of new interferometric data of NGC 4151, discussed in context with the results from recent dust reverberation, spectro-photometric and interferometric campaigns. The complete data set gives a complex picture, in particular the measured visibilities from three different nights appear to be rather independent of the nuclear luminosity. The KI data alone indicate two scenarios: the  $K$ -band emission is either dominated to  $\sim 90\%$  by size scales smaller than  $20\ \text{mpc}$ , which falls short of any dust reverberation measurement in NGC 4151 and of theoretical models of circumnuclear dust distributions. Or contrary, and more likely, the  $K$ -band continuum emission is dominated by hot dust ( $\gtrsim 1300\ \text{K}$ ) at linear scales of about  $50\ \text{mpc}$ , depending on the detailed observed morphology. This is roughly consistent with the expectations from circumnuclear, dusty radiative transfer models, and spectro-photometric modeling. The data do not support a dust emission size scale which follows the strong nuclear variability of NGC 4151. Instead variable nuclear activity and changing dust heating efficiency need to be combined to explain the observations.

---

<sup>1</sup>current address: Max-Planck-Institut für Astronomie, Königstuhl 17, D-69117 Heidelberg, Germany  
jpott@mpia.de, herbst@mpia.de

<sup>2</sup>Div. of Astronomy & Astrophysics, University of California, Los Angeles, CA 90095-1547  
malkan@astro.ucla.edu, ghez@astro.ucla.edu

<sup>3</sup>W. M. Keck Observatory, California Association for Research in Astronomy, Kamuela, HI 96743  
jwoillez@keck.hawaii.edu

<sup>4</sup>Dept. of Physics and Astronomy, University of Kentucky, Lexington, KY 40506-0055  
moshe@pa.uky.edu

<sup>5</sup>Institute of Geophysics and Planetary Physics, University of California, Los Angeles, CA 90095-1565

<sup>6</sup>Instituto de Astrofísica de Andalucía - CSIC, Camino Bajo de Huétor, 50, 18008 Granada, Spain  
rainer@iaa.es

*Subject headings:* ...

## 1. Introduction

Nearby Active Galactic Nuclei (AGN) are rosetta stones to understand the astrophysics close to an actively accreting super-massive black hole. Sub-parsec resolution is required to identify answers to the key questions of AGN physics: (i) How does galactic material flow down to the accretion disk to feed luminosities close to the Eddington limit? (ii) Which role do play outflows and jets in the energetic interconnection between the AGN and its host? and (iii) Are AGN of different luminosity intrinsically similar? Studying the spectral energy distribution of quasars and type 1 AGN from the optical to the far-infrared reveals remarkably similar SED shapes, suggesting similar physics (Edelson & Malkan 1986; Sanders et al. 1989; Kobayashi et al. 1993; Riffel et al. 2006). Therefore, resolving astrophysical phenomena in nearby AGN enables to better understand farther, unresolved nuclei, and to gauge correlations between nuclear luminosity and properties of the surrounding circumnuclear environment. Being one of the brightest AGN on the sky, NGC 4151 reveals this unique potential of nuclei closer than a few tens of Mpc’s in numerous publications.

In this article, we concentrate on the origin of the near-infrared (NIR) emission of NGC 4151, and its relation to the nuclear luminosity. NIR-AGN emission is characterized by a steep decline from optical wavelengths down to about  $1 \mu\text{m}$ , and on the long wavelength side by the quick rise of a separate IR emission bump peaking at about  $3 \mu\text{m}$  (Edelson & Malkan 1986; Kobayashi et al. 1993). The origin of this NIR excess has been discussed throughout the past four decades (probably one of the first were Pacholczyk & Weymann 1968; Rees et al. 1969). While it is not in question that the original power originates in the accretion disk, it is uncertain if the NIR emission excess derives directly from nuclear emission processes, or if mostly dust outside the broad line region (BLR) re-radiates the nuclear emission (Edelson & Malkan 1986; Edelson et al. 1988; Barvainis 1987, 1992). The proper measurement of the nuclear near-infrared emission (and its discrimination from dust-re-processed light) is crucial to derive the intrinsic SED of accreting supermassive black holes (SMBH) in the centers of galaxies and to understand the radiative processes involved.

Even at the relatively large linear scale of NGC 4151 ( $\sim 65 \text{ mpc} / \text{mas}^1$ ), the accretion disk itself and the surrounding BLR are too small to be spatially resolved by the current generation of optical or infrared telescopes or interferometers (Bentz et al. 2006). However, the circum-nuclear dust distribution is now within reach of observations with infrared telescope

---

<sup>1</sup>based on the  $z \sim 0.00332$ , and  $H_0 = 73 \text{ km s}^{-1} \text{ Mpc}^{-1}$

arrays at sub-50 mas angular resolution (Swain et al. 2003; Wittkowski et al. 2004; Jaffe et al. 2004). Mid-infrared data of the VLT interferometer typically find in Seyfert nuclei  $10\ \mu\text{m}$  emission sizes of a few parsecs (Tristram et al. 2009; Burtscher et al. 2009; Raban et al. 2009). Dust plays an exceptional role among the circumnuclear components. It is not only assumed to significantly contribute to the near-to-mid-infrared continuum radiation of an AGN. Also, a non-spherically symmetric dust distribution is widely assumed to explain the type 1 / 2 dichotomy of AGN emission line spectra. Radiative transfer models of clumpy distributions of dust clouds extending out of the equatorial plane are currently the favored explanation of the steadily increasing amount of observational data (Barvainis 1987, 1992; Schartmann et al. 2005; Hönig et al. 2006; Nenkova et al. 2008a,b; Hönig & Kishimoto 2009). In the following we refer to the dust distribution as *torus*, keeping in mind that its detailed morphology is rather uncertain, might not resemble closely a smooth torus.

It is currently an open debate, how the findings and models at MIR wavelengths connect to the innermost hot dust, which is expected to contribute to the continuum emission at  $2\ \mu\text{m}$ . Mor et al. (2009) argue for a spatially and chemically distinct inner component, based on  $2 - 35\ \mu\text{m}$  spectra. Also, the interferometric MIR data of NGC 4151 appears to reject that the nuclear flux at  $10\ \mu\text{m}$  is dominated by the outer, cooler part of the same structure, which dominates the  $2\ \mu\text{m}$  continuum (Burtscher et al. 2009). Such results discourage simple attempts to unify the dust emission structures around AGN, and suggest multi-component models, or at least a significant change of dust composition and grain size distribution with the radial distance to the central engine (Schartmann et al. 2005; Kishimoto et al. 2009a).

We report in this letter on first results of a new campaign using the Keck Interferometer (KI) to add observational constraints to the origin of the NIR continuum of NGC 4151. The 85 m baseline and the sensitivity of the KI is adequate to resolve the linear distances of order 30-200 mpc around NGC 4151 which matches the dust sublimation radius for this source. Recent sensitivity improvements of the KI (Wizinowich et al. 2006, <sup>2</sup>) enabled us to repeat the early Swain et al. KI measurement, although the variable nucleus of NGC 4151 has been at a significantly fainter state during the time of observation. After a description of the observations (Sect. 2), we discuss our findings and the implications on the interpretation of the combined visibility data set (Sect. 3). The concluding remarks in Sect.4 summarize our current results and give a brief outlook on the project.

---

<sup>2</sup>Current KI performance numbers are given at the website of NASA Exoplanet Science Institute (NEXSCI): <http://nexsci.caltech.edu/software/KISupport/v2/v2sensitivity.html>

## 2. Observations

The 85 m baseline of the Keck Interferometer (KI) is oriented  $38^\circ$  east of north (Colavita et al. 2004; Wizinowich et al. 2004). We used the  $K'$ -band (2-2.4  $\mu\text{m}$ )  $V^2$  continuum mode. All data shown here are from the white-light channel of the beam combiner, observed at an effective wavelength of 2.18  $\mu\text{m}$ . The observations were conducted on Dec. 15, 2008 (UT), details appear in Table 1. We followed standard observing and data reduction procedures (see Sect. 3.2 in Colavita et al. 2003, and references therein). KI data are provided to the observer in a semi-raw state, and still require division by the system visibility (or visibility transfer function), which is estimated by observing unresolved calibrators, close in space and time (typical numbers for *close* are  $\lesssim 10^\circ$  and  $\lesssim 0.5$  hr). The provided raw visibilities ( $V^2$ ) are weakly dependent on the  $K$ -band flux of the observed target, so we chose calibrators of similar  $K$ -band magnitude (Table 2). Our typical scanlength, leading to one visibility point, is 200 sec.

A reliable data calibration is indicated by stable system visibility and the flux ratios between both telescope beams over the nights. To estimate and apply the system visibility, we used the wb/nbCalib-software suite by NEXSCI. We use the standard deviation over the about 25 blocks, which making up the 200 s scan, as a first estimate of the uncertainties of each data point. The resulting statistical noise in the calibrated visibility measurement is 0.01, proving the good observing conditions of the night. This is a good measure for the differential intranight visibility accuracy. Long-term monitoring of KI data shows that the absolute calibration precision of the data from night to night is at least 0.03<sup>3</sup>. Therefore, we use 0.03 as precision for our calibrated visibilities and the following analysis, since we aim at comparing our results with other campaigns.

## 3. Discussion of the results

The calibrated visibilities are plotted in Fig. 1 versus hour angle and projected baseline length. Previously published data by Swain et al. (2003) are added. It is apparent that the different interferometry campaigns measured very similar visibilities. Taking into account, that the absolute  $V^2$ -calibration accuracy between different runs is with  $\lesssim 0.03$  lower than the differential accuracy within a run (the latter shown as error bars for the new measurements) all visibilities are consistent with each other. This is interesting given the significant brightness variation of the total  $K$ -band flux, seen by the KI 50 mas diameter aperture, and

---

<sup>3</sup><http://nexsci.caltech.edu/software/KISupport/v2/v2sensitivity.html>

Table 1: Observing log.

Target	date (UT)	H.A. <sup>a</sup> [hr]	$u, v$ <sup>b</sup> [m]	proj. B <sup>b</sup> [m, deg(EofN)]	calibrators [from Tab 2]	$V^2$ [calib.] <sup>c</sup>
NGC 4151	Dec.15,2008	-1.3	(56.4, 51.6)	(76.4, 47.5)	1,2	0.85
	Dec.15,2008	-1.1	(56.0, 54.0)	(77.8, 46.0)	1,2	0.84

<sup>a</sup>Hour angle

<sup>b</sup>The  $u, v$ -coordinates, given here in meters, are the baseline length (B) projected onto the line of sight.  $u$  points East,  $v$  points North. They are equivalent to polar values of the projected baseline, given in the next column in meters, and degrees East of North.

<sup>c</sup>The *absolute* calibration precision is at least 0.03, which is shown in Fig. 1 and should be used if comparing these values with results from different nights and observing campaigns. The *differential* intranight visibility accuracy is 0.01, based on the statistical scatter of the measurements.

Table 2: Properties of the interferometric calibrator stars used for calibration of the instrumental transfer function during data reduction.

#	Calibrator	$V/H/K$ <sup>(a)</sup>	Spec. Type <sup>(a)</sup>	Ang. diameter (mas) <sup>(b)</sup>
1	HIP58819	10.9/8.5/8.4	K0III	$0.11 \pm 0.03$
2	HD109691	8.9/8.9/8.9	A0V	$0.04 \pm 0.02$

<sup>a</sup>from SIMBAD

<sup>b</sup>bolometric diameter fit from the NEXSCI getCal tool.

Note. — Calibrator stellar diameters significantly smaller than 0.5 mas, are unresolved by the KI. The statistical errors given here for the bolometric diameter fit to a black body likely slightly underestimate systematic errors of the NIR diameter of stars, but even 0.2 mas uncertainties in the diameter would not change the visibility calibration.

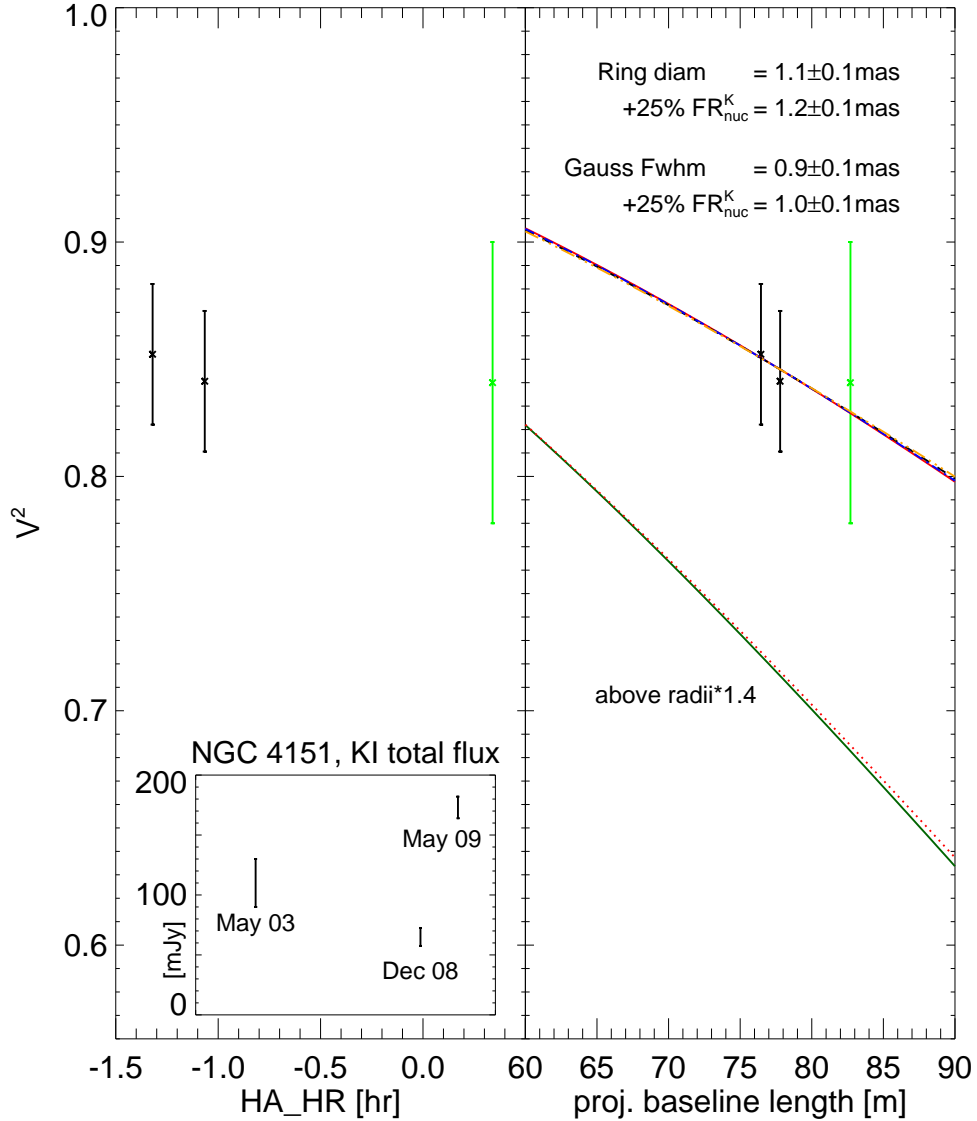


Fig. 1.— Calibrated visibility data from our observations (Dec 08, black) and from Swain et al. (2003, May 03, green). As inset in the left panel, the KI total fluxes of the measurements are shown, together with the respective value from a new KI dataset (Kishimoto et al. 2009b). The right panel shows the data versus the projected baseline length.  $\chi^2$  minimized model fits are overplotted. The best fit diameters are given. A compact flux contribution on the order of 25 % (labelled  $FR_{\text{nuc}}^K$ ) does not alter the results significantly. The lines below the data points in the right panel are the same models with an increased size according to a doubling of the nuclear illumination power. Such models do not fit the data (see Sect. 3.1 for details).

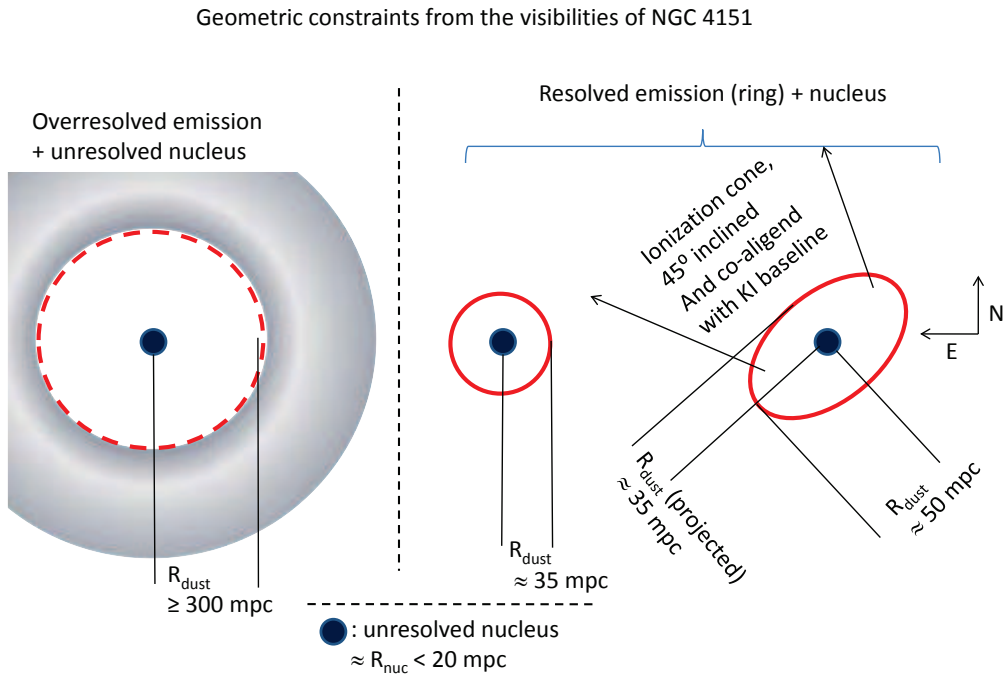


Fig. 2.— Sketches (not to scale) of the geometric constraints on the extended  $K$ -band emission of NGC 4151, seen through the 50 mas spatial filter of the Keck interferometer. Details are given in Sect. 3. Note that the overresolved emission might be diffuse, or more spherically than drawn, but the emission needs to originate from centronuclear radii larger than 300 mpc to be completely resolved out, and to not contribute to the  $V^2$ -budget.

plotted as inset in the left panel of Fig. 1.

We recapitulate three interpretation facts of visibility data sets similar to the presented one. The respective models essentially consist of a variable fractional amount of (unresolved) nuclear emission ( $FR_{\text{nuc}}^K = 0 - 1$ ) along with resolved (overresolved) emission at (beyond) centro-nuclear radii  $R_{\text{dust}}$  (Fig. 2). We simply refer to the extended component as dust, being the most likely origin of it.

(1) Already a single visibility below unity shows that the observed source is not completely unresolved (compact) and  $FR_{\text{nuc}}^K$  is smaller than unity. The most compact brightness distribution, still consistent with the data, would put  $FR_{\text{nuc}}^K \sim 90\%$  of the flux at radii smaller than  $0.35''$  (20 mpc) below the resolution limit of the KI ("point source"), and the remainder of the flux outside of  $R_{\text{dust}} \sim 300$  mpc to be completely resolved out. Since radii of about 20 mpc are significantly smaller than the dust sublimation radius in NGC 4151, this scenario would suggest that the  $K$ -band emission is dominated by hot, and potentially partially non-thermal nuclear emission from the innermost accretion disk zone. But the derivation of  $FR_{\text{nuc}}^K$  from a few visibilities is degenerate. Reducing  $FR_{\text{nuc}}^K$  requires only to shrink  $R_{\text{dust}}$  to stay consistent with the data. The visibility alone does not constrain  $FR_{\text{nuc}}^K$  any further than being smaller than 0.9. However, recent spectro-photometric and NIR-polarimetric data appear to limit  $FR_{\text{nuc}}^K$  to less than 25%, and thus suggest a domination of the central  $K$ -band flux by moderately warm thermal emission ( $\sim 1500$  K), likely from circumnuclear dust clouds (see the detailed discussions and references pro and against the dominating origin of the  $K$ -band emission in Seyfert 1 nuclei in Barvainis 1987; Riffel et al. 2009; Kishimoto et al. 2009a,b). Since our data is consistent with these findings, we assume  $FR_{\text{nuc}}^K \lesssim 0.25$ .

(2) The high differential stability of repeated visibility measurements from a single night give a new constraint. Both recent KI datasets from our observations and from Kishimoto et al. (2009b) show a marginally decreasing visibility trend with increasing projected baseline length. This means that the interferometer actually resolves the emission structure, and the order of magnitude of  $R_{\text{dust}}$  can be estimated. To translate visibilities into size scales, a simple model of the extended emission is required. Gaussians and rings fit the data equally well, and give the same  $R_{\text{dust}}$  of 35 mpc ( $0.5 \cdot \text{FWHM} \approx R_{\text{ring}} = 0.55 \pm 0.1$  mas, Fig. 1). This size estimate is largely unaffected by an  $FR_{\text{nuc}}^K \lesssim 25\%$ , or by the radial extension of the ring as long as the ring radius is larger than its extension (Fig. 1). The key difference between both models is, that the Gaussian not only defines a size scale, but at the same time constrains the emitting *area*. The fitted FWHM translates into a solid angle of  $0.92 \text{ mas}^2$ . However, a brightness temperature calculation rejects a smooth Gaussian-like emission surface profile. Assuming a black body temperature of 1300 K, this surface would result in about 500 mJy. This is about a factor of 2.5-10 larger than the measured dusty  $K$ -band emission of NGC 4151, depending on its status of nuclear activity. If the



dust emission is optically thick, this discrepancy means that the radiating surface area is significantly smaller than the solid angle of the fitted Gaussian. If we were to shrink the FWHM of the Gaussian to match the observed fluxes, the resulting increased visibilities would overshoot over the data. Higher dust temperatures would strengthen this argument against a smooth Gaussian brightness distribution. Thus we conclude that the black body component, apparent in the spectro-photometry, is not produced by a rather spherical dust distribution (which would resemble a Gaussian in projection). The planar geometry of the ring model seems more reasonable. This matches the expectation for observing a type 1 AGN. Optically thick clouds as used in modern torus models would reduce the radiating surface as well (without changing the  $R_{\text{dust}}$  estimate) but the ring morphology also appears more reasonable due to the lack of significant extinction towards the very nucleus (Lacy et al. 1982).

(3) The  $R_{\text{dust}}$  estimate from the previous paragraph assumes a face-on, circular dust distribution. However, given the single telescope baseline, the size constraints of KI-data are mostly one-dimensional along the position angle of the baseline (about  $40^\circ$ ). The resolved source could be substantially larger along the orthogonal (SE-NW) direction. In fact, the baseline position angle roughly co-aligns with the ionization cone axis of symmetry of NGC 4151. Das et al. (2005); Riffel et al. (2009) report position, opening and line-of-sight inclination angles of the cone to be  $\sim 60^\circ$ ,  $\sim 70^\circ$ , and  $\sim 45^\circ$ . If the circumnuclear dust, seen as extended component by the interferometer, is responsible for the formation of the ionization cone, the opening angle translate into a torus half-height of 0.7 times the inner radius. This matches with our thin ring model approach, if the extended  $K$ -band emission is dominated by the hottest dust exposed to direct nuclear illumination. The position and inclination angle however indicate, that the KI measures  $R_{\text{dust}}$  close to the (projected) minor axis, and that the 3d inner torus radius is  $\sim 50$  mpc instead. The significant inclination of the nuclear axis of symmetry, indicated by the inclination of the ionization cone, is supported by the time-variable, spectral classification of NGC 4151 as Seyfert 1.5 - 1.8 (Shapovalova et al. 2008).

### 3.1. Variable torus size or variable illumination

In general, both  $V$ -to- $K$ -continuum reverberation and NIR interferometric measurements of nearby AGN appear to confirm a  $L^{0.5}$ -dependence of the extended  $K$ -band emission size on the nuclear illumination luminosity (Suganuma et al. 2006; Kishimoto et al. 2009b). In addition, the NIR SED bump can be fitted consistently with a black body profile of about 1500 K, for AGN samples covering orders of magnitude in nuclear power (Kobayashi et al.

1993). These are strong arguments for that the  $K$ -band is dominated by thermal dust emission close to the sublimation limit. The strong nuclear emission variability of NGC 4151 by several 100 % on year-timescales makes it an ideal target for studying the detailed relation between the nuclear emission and the dust emission size. Given an estimated dust size scale of tens of mpc, it would require unreasonable fast dust bulk motion (at 0.1 c), if the dust size were to follow such fast and large illumination variations. Therefore, cyclic dust grain destruction and formation was suggested to explain the observed infrared flux variations (Barvainis 1992) and the large scatter and poor  $L^{0.5}$ -dependence in the dust reverberation size estimates of NGC 4151 (Koshida et al. 2009).

While such dust processing avoids the need for unphysically large bulk motion, occurring dust sublimation would still increase the apparent dust emission size, seen by the interferometer. For the first time, we can compare these claims against a multi-epoch visibility dataset of the AGN, taken at different brightness states (see inset in Fig. 1). We compared the published data with our measurements and derive a flux difference of nearly a factor of two, falling well within the total observed range of flux variations. Due to the 50 mas spatial filtering of the fringe tracking camera, the precision of the flux calibration of KI data is limited by its dependence on the stability of the Strehl ratio, but our data are stable at the 10% level. Even such rather large uncertainties on the total flux measurement leave no doubt that NGC 4151 was significantly brighter in 2003, and in May 09, than during our campaign. In particular we are confident that the total flux variation is not induced by different Strehl due to a direct comparison of our measurement against the archived KI-data, and due to very good and stable sky conditions during our observing night (visible seeing at about 0.5”).

Assuming a simple  $L^{0.5}$  scaling, the flux variation by a factor two would result in a size increase by a factor of 1.4 . In Fig. 1 we overplotted our best fit ring models, increased by 1.4. Those increased size scales do not fit the old data set. Vice versa, ring-models from the Swain publication, decreased by 1.4 do not fit the new data. This finding remains significant down to a flux increase of only 25 %, which is the minimum flux increase consistent with our photometric estimates. Similarly the data from Kishimoto et al. (2009b) show a flux increase of three with respect to our measurements, but no respectively large visibility decrease.

A closer look to the results of the spectro-photometric modeling and the KI-observations suggest a scenario different from the luminosity-size scaling. Kishimoto et al. (2007) measured a significantly higher nuclear flux contribution to the  $K$ -band at a brighter state of the nucleus than during the observation of Riffel et al. (2009) (20-25% with respect to 10%), although both teams fitted in comparable ways very similar black body temperatures to the NIR-emission. The comparison of the two new precise visibility measurements reveal a small

$V^2$ -offset of 0.04 at the same angular resolution (projected baseline length) between our and the Kishimoto09 data. This difference would result from changing  $FR_{\text{nuc}}^K$  between both measurements from the 10 % level in Dec 08 to the 20 % level in May 09. Note that the accuracy of the  $R_{\text{dust}}$  estimation in the previous section does not suffice to distinguish between such a subtle  $V^2$ -difference due to the geometric model assumption.  $R_{\text{dust,projected}} \approx 35$  mpc is an order of magnitude result, which fits all three datasets and excludes a strict  $L^{0.5}$  scaling. But here we compare model-free the visibilities, and the small difference, slightly larger than the conservative internight accuracy estimate of 0.03, can be accommodated by a change of the compact  $FR_{\text{nuc}}^K$ , without further assumptions on the structure of the extended emission.

A variation of the fractional  $FR_{\text{nuc}}^K$  cannot be explained alone by a varying line-of-sight extinction towards the nucleus (e.g. due to passing clouds), because such an apparent luminosity change should not result in the observed time-correlated dust emission change. In addition, an optical polarization reverberation study of NGC 4151 suggests electron scattering at the low-ionization BLR as the dominant origin of the polarization (Gaskell et al. 2007). The authors suggest that the observed variation of the percentage polarization on year-timescales would refer to structural changes of the scatterer. However, both the variability of  $FR_{\text{nuc}}^K$  and of the optical polarization percentage could also be explained by a time variable orientation of an anisotropic nuclear illumination source, pointing to various loci of fixed scattering and dusty emission structures. Also the strong nuclear continuum variability itself could be explained by such a "lighthouse effect".

Since the interferometric data suggest a rather flux-independent dust emission size, we find two interesting implications of the here derived intrinsic  $R_{\text{dust}}$  ( $\sim 50$  mpc, see Sect. 3). It equals 60 days of light travel, and thus matches the first four dust reverberation measurements of Koshida et al. (2009). Because these earlier dust reverberation measurements span already a factor of six in optical luminosity, they also suggest a fixed dust emission size. The first KI measurement by Swain et al. (2003) is quasi-contemporaneous with one of these dust reverberation measurements. Thus both methods appear to agree very well. However, the former authors report on four subsequent, significantly smaller reverberation size estimates, the shortest being  $\sim 30$  mpc only. Although there is no interferometric data at those epochs, the arguments given above rather suggest that  $FR_{\text{nuc}}^K$ -variability is the origin of these smaller size estimates instead of a true shrinkage of the 50 mpc sized emission structure. A increased  $FR_{\text{nuc}}^K$  implies a different dust heating efficiency, for instance due to a lower covering factor and larger dust grains sizes. These parameters most likely vary in favor of larger  $FR_{\text{nuc}}^K$  for dust closer to the nucleus. Also, reverberation size estimates are biased to the innermost responding material (Gaskell & Sparke 1986).

This implies that dust reverberation sizes may often underestimate the location of the

bulk of the circumnuclear dust, which dominates the  $K$ -band emission. Indeed, if we use our  $R_{\text{dust}}$  for NGC 4151, three of the four interferometric  $R_{\text{dust}}$  estimates of the AGN, observed by Kishimoto et al. (2009b), exceed the  $L^{0.5}$ -fit of the reverberation size by factors of about  $2 \pm 0.5$ . The direct interferometric  $R_{\text{dust}}$  estimate appears as the more robust measurement of the average location of the bulk of the warm circumnuclear dust (if projection ambiguities are well constrained), whereas the rapidly changing smallest reverberation sizes are probably tracing the momentary illumination of some very hot dust clouds closest to the nucleus.

#### 4. Conclusions

The results of a new interferometric NIR observing campaign of NGC 4151 are presented. Although this time in a 2-3 times fainter state, we managed to re-observe the AGN with the Keck Interferometer thanks to recent sensitivity improvements. The interferometric visibilities and size estimates were compared to previously published interferometric and single telescope data. The current KI datasets suggest that the major part of the radiation originates in a (possibly inclined) toroidal structure of an intrinsic radius of about 50 mpc, comparable to  $V$ -to- $K$ -continuum reverberation measurements, without constraining the morphology in further detail.

Our dataset enables for the first time to study the flux dependence of near-infrared interferometric visibilities of an AGN. The observations show that NIR-interferometry on  $K \sim 10$  mag AGN are now feasible at a high precision of a few percent. We did not detect a significant visibility dependence on more than doubling the  $K$ -band emission of NGC 4151. This supports the notion, that, for an individual AGN, the size of its circumnuclear NIR emission structure does not strictly depend on the respective momentary nuclear luminosity. The direct interferometric size estimates appear to be more robust estimates of the average location of the dust than continuum reverberation estimates. Being flux-independent, this average location probably relates to the sublimation radii of the AGN at its high activity state. Future dust reverberation campaigns, contemporaneous to direct interferometric measurements are highly desirable to study the circumnuclear NIR emission region, to correctly interpret the reverberation measurements, and to investigate apparent changes in the dust illumination, heating efficiency, and covering factors.

We are grateful to the excellent KI team at WMKO and NExSci for making these observations a success. K. Meisenheimer and L. Burtscher contributed helpful discussions. The data presented herein were obtained at the W.M. Keck Observatory, which is operated as a scientific partnership among the California Institute of Technology, the University of

California and the National Aeronautics and Space Administration. The Observatory was made possible by the generous financial support of the W.M. Keck Foundation. The authors wish to recognize and acknowledge the very significant cultural role and reverence that the summit of Mauna Kea has always had within the indigenous Hawaiian community. We are most fortunate to have the opportunity to conduct observations from this mountain. The Keck Interferometer is funded by the National Aeronautics and Space Administration as part of its Navigator program. This work has made use of services produced by the NASA Exoplanet Science Institute at the California Institute of Technology. This research has made use of the SIMBAD database, operated at CDS, Strasbourg, France. This research has made use of the NASA/IPAC Extragalactic Database (NED) which is operated by the Jet Propulsion Laboratory, California Institute of Technology, under contract with the National Aeronautics and Space Administration.

*Facilities:* Keck:I (), Keck:II ()

## REFERENCES

- Barvainis, R. 1987, ApJ, 320, 537
- Barvainis, R. 1992, ApJ, 400, 502
- Bentz, M. C., Peterson, B. M., Pogge, R. W., Vestergaard, M., & Onken, C. A. 2006, ApJ, 644, 133
- Burtscher, L., Jaffe, W., Raban, D., Meisenheimer, K., Tristram, K. R. W., Röttgering, H. 2009, ApJ, 705, L53
- Colavita, M., et al. 2003, ApJ, 592, L83
- Das, V., et al. 2005, AJ, 130, 945
- Edelson, R. A., & Malkan, M. A. 1986, ApJ, 308, 59
- Edelson, R. A., Gear, W. K. P., Malkan, M. A., & Robson, E. I. 1988, Nature, 336, 749
- Gaskell, C. M., & Sparke, L. S. 1986, ApJ, 305, 175
- Gaskell, C. M., Goosmann, R. W., Merkulova, N. I., Shakhovskoy, N. M., & Shoji, M. 2007, arXiv:0711.1019
- Hönig, S. F., Beckert, T., Ohnaka, K., & Weigelt, G. 2006, A&A, 452, 459

- Hönig, S. F., & Kishimoto, M. 2009, arXiv:0909.4539
- Jaffe, W., et al. 2004, *Nature*, 429, 47
- Kishimoto, M., Antonucci, R., & Blaes, O. 2005, *MNRAS*, 364, 640
- Kishimoto, M., Hönig, S. F., Beckert, T., & Weigelt, G. 2007, *A&A*, 476, 713
- Kishimoto, M., Antonucci, R., Blaes, O., Lawrence, A., Boisson, C., Albrecht, M., & Leipski, C. 2008, *Nature*, 454, 492
- Kishimoto, M., Hönig, S. F., Tristram, K. R. W., & Weigelt, G. 2009, *A&A*, 493, L57
- Kishimoto, M., Hoenig, S. F., Antonucci, R., Kotani, T., Barvainis, R., Tristram, K. R. W., & Weigelt, G. 2009, *A&A Letters in press*, arXiv:0911.0666
- Kobayashi, Y., Sato, S., Yamashita, T., Shiba, H., & Takami, H. 1993, *ApJ*, 404, 94
- Koshida, S., et al. 2009, *ApJ*, 700, L109
- Lacy, J. H., et al. 1982, *ApJ*, 256, 75
- Minezaki, T., Yoshii, Y., Kobayashi, Y., Enya, K., Suganuma, M., Tomita, H., Aoki, T., & Peterson, B. A. 2004, *ApJ*, 600, L35
- Mor, R., Netzer, H., & Elitzur, M. 2009, *ApJ*, 705, 298
- Nagar, N. M., & Wilson, A. S. 1999, *ApJ*, 516, 97
- Nenkova, M., Sirocky, M. M., Ivezić, Ž., & Elitzur, M. 2008a, *ApJ*, 685, 147
- Nenkova, M., Sirocky, M. M., Nikutta, R., Ivezić, Ž., & Elitzur, M. 2008b, *ApJ*, 685, 160
- Netzer, H. 2009, *ApJ*, 695, 793
- Onken, C. A., et al. 2007, *ApJ*, 670, 105
- Pacholczyk, A. G., & Weymann, R. J. 1968, *AJ*, 73, 870
- Raban, D., Jaffe, W., Röttgering, H., Meisenheimer, K., & Tristram, K. R. W. 2009, *MNRAS*, 394, 1325
- Rees, M. J., Silk, J. I., Werner, M. W., & Wickramasinghe, N. C. 1969, *Nature*, 223, 788
- Riffel, R., Rodríguez-Ardila, A., & Pastoriza, M. G. 2006, *A&A*, 457, 61

- Riffel, R. A., Storchi-Bergmann, T., & McGregor, P. J. 2009, *ApJ*, 698, 1767
- Ruiz, M., Young, S., Packham, C., Alexander, D. M., & Hough, J. H. 2003, *MNRAS*, 340, 733
- Sanders, D. B., Phinney, E. S., Neugebauer, G., Soifer, B. T., & Matthews, K. 1989, *ApJ*, 347, 29
- Schartmann, M., Meisenheimer, K., Camenzind, M., Wolf, S., & Henning, T. 2005, *A&A*, 437, 861
- Schmitt, H. R., & Kinney, A. L. 1996, *ApJ*, 463, 498
- Shapovalova, A. I., et al. 2008, *A&A*, 486, 99
- Suganuma, M., et al. 2006, *ApJ*, 639, 46
- Swain, M., et al. 2003, *ApJ*, 596, L163
- Tristram, K. R. W., et al. 2009, *A&A*, 502, 67
- Wandel, A., Peterson, B. M., & Malkan, M. A. 1999, *ApJ*, 526, 579
- Wittkowski, M., Kervella, P., Arsenault, R., Paresce, F., Beckert, T., & Weigelt, G. 2004, *A&A*, 418, L39
- Wizinowich, P., et al. 2006, *Proc. SPIE*, 6268,